

Effect of Surface Layer Stochasticity on Seismic Ground Motion Coherence and Strain Estimates

by

A. Zerva

Department of Civil and Architectural Engineering, Drexel University,
Philadelphia, PA 19104, USA

and

T. Harada

Faculty of Engineering, Miyazaki University, Miyazaki 889-21, Japan

Abstract

The significance of stochasticity in the characteristics of the surface layers of a site to the resulting spatial variation of seismic ground motions and the seismic ground strains is investigated. For this purpose, an analytical site-specific model is developed. The model approximates the site topography by a horizontally extended layer with random characteristics overlaying a half-space (bedrock). The spatial variation of the incident motion at the bedrock-layer interface incorporates the effects of the loss of coherence of the motions at increasing separation distances and their propagation in the bedrock; the site contribution to the spatial variation of the surface motions results from the vertical transmission of shear waves through the stochastic layer. It is shown, in an example application of the approach, that the spatial coherence of the motions on the ground surface is similar to that of the incident motion at the bedrock-layer interface except at the predominant frequency of the layer, where it decreases considerably. It is also shown that, for soft soil conditions, the layer stochasticity controls seismic ground strains. In the absence of spatially recorded seismic data at a site, the approach can be utilized for the description of the spatial variation of the motions in the seismic response analysis of buried and above-ground lifelines.

November 17, 1996

revised May 10, 1997

accepted for publication in *Soil Dynamics
and Earthquake Engineering* - in press

1 Introduction

The seismic resistant design of conventional “point” structures requires information on the time variation of the seismic ground motions at a single location on the ground surface; because the dimensions of such structures are relatively small compared to the wavelengths of the seismic motions, it can be assumed that the ground excitations over the entire foundation area are essentially the same. This is not the case, however, for the seismic response of lifelines. Lifelines, such as pipelines and bridges, extend over long distances parallel to the ground, and their supports undergo different motions during earthquakes. The differential motion or the spatial variation of the seismic ground motions may induce significant additional forces in the structures than the ones obtained if it is assumed that the motions at all supports are identical.

The spatial variation of the seismic ground motions is caused by their apparent propagation on the ground surface and the change in their shape (loss of coherence) at various locations. It is, generally, obtained from the analysis of recorded data at dense instrument arrays, such as the SMART-1 array in Lotung, Taiwan (e.g., [2], [3], [9], [10], [12], [17], [18], [34]); most of these analyses consider the strong motions of the direct S-wave window. It has been recognized that the spatial variation of the seismic ground motions can be described by a function exponentially decaying with separation distance and frequency (e.g., [3], [25], [34]). However, various expressions and different degrees of exponential decay appear to fit data recorded at the same site for different earthquakes or at different sites. It has not been established yet which spatial variability model is the more appropriate for the seismic analysis of lifelines. Furthermore, the choice of any particular model (mathematical expression and degree of exponential decay) in the seismic response analysis of lifelines has a significant effect on the resulting structural response: the degree of correlation in the spatial variation at low frequencies controls differential ground displacements, seismic strains and the quasi-static response of lifelines, whereas the degree of the exponential de-

cay at higher frequencies controls the dynamic response of above-ground lifelines [39], [40]. Consequently, a major difficulty in the evaluation of the seismic response of these extended structures is the selection of an appropriate spatial variability model for the site under consideration, when spatially recorded seismic data are not available. Thus, there is a need for reliable site-specific, analytical and/or empirical models for the spatial variation of the seismic ground motions to be used in the seismic resistant analysis and design of lifelines.

Somerville *et al* [28] proposed a model, in which they attribute spatial variability to the wave propagation effect, the finite source effect, the effect of scattering of the seismic waves as they propagate from the source to the site, and the local site effects. Schneider *et al* [25] considered that the spatial variability is the product of two terms, the first corresponding to source and wave passage effects and the second to the scattering of the waves from the source to the ground surface. In a recent study, Spudich [29] indicated that the main contributors to the spatial variation of the seismic motions are the wave passage effects, the free surface boundary conditions, which may introduce surface waves, and the site conditions, which may introduce spatially variable delays in the arrival of the waves from the bedrock to the surface as well as spatially variable site effects; Spudich [29], based on a review of seismological observations, also suggested that the effect of source finiteness is minimal. Der Kiureghian [7] has recently developed a stochastic model, in which the total spatial variation of the seismic motions is composed of terms corresponding to wave passage effects, effects of loss of coherence in the bedrock motion, and site response contribution.

This work deals also with the analytical evaluation of the spatial variation of the seismic motions. Contrary to current approaches, that consider fully deterministic layer characteristics for the site response contribution to spatial variability, the present analysis investigates the effect of layer stochasticity in the resulting seismic ground motions. It attributes the total spatial variation of the strong, shear-wave motions to the wave passage effect, the scattering of the waves from the source to the site, and the local site conditions. Based

on Spudich's [29] observations, the effect of source finiteness is not taken into consideration. The scattering of the shear waves from the source to the site is represented by a commonly used model for the loss of spatial coherence in seismic ground motions. The wave passage effect is represented by a phase difference term, i.e., the seismic time history propagates with a constant velocity on the ground surface, as is, generally, the case for the strong S-wave window of the motions. The approach concentrates on the site response effect, which is approximated by one-dimensional, shear wave propagation through a random layer. Thus, the methodology is applicable to sites which can be approximated by horizontal layers without dramatic changes in their topography and for the strong motion S-wave window. The contributions of the various factors to the spatial variation of the surface motions and the resulting seismic ground strains are examined for an example site. It is shown that variabilities in the soil characteristics can significantly reduce the degree of correlation of the seismic motions at the stochastic layer predominant frequency and significantly increase the value of seismic ground strains. Thus, stochasticity in the soil characteristics ought to be incorporated in spatial variability models. In the absence of spatially recorded seismic data at a site, the results of the present approach can be used as a realistic approximation for the description of spatially variable seismic ground motions in the seismic response analysis of above-ground and buried lifelines.

2 Seismic ground displacements in homogeneous stochastic layered media

2.1 Evaluation of seismic ground motions

Consider an elastic half-space (bedrock) underlying a horizontally extended layer with stochastic properties; the coordinate along the depth of the layer is indicated by z and that along the ground surface by x . The total layer thickness is constant and equal to H . Within the layer the soil characteristics (shear modulus $G(x, z)$ and mass density $\rho(x, z)$)

vary randomly along the horizontal coordinate as:

$$G(\mathbf{x}, z) = G_z(z)[1 + f_G(x)] \quad (1)$$

and

$$\rho(\mathbf{x}, z) = \rho_z(z)[1 + f_\rho(x)] \quad (2)$$

where, $G_z(z)$ and $\rho_z(z)$ represent the mean values of $G(\mathbf{x}, z)$ and $\rho(\mathbf{x}, z)$, respectively, and are deterministic functions of z , and $f_G(x)$ and $f_\rho(x)$ represent stochastic fields with zero mean along the horizontal coordinate x .

The incident seismic motion at the bedrock-layer interface, $u_b(x, t)$, is represented by stationary random shear waves. The displacement time history at any location (x, z) within the layer is the superposition of the incident displacement at the bedrock-layer interface, $u_b(x, t)$, and the relative displacement between the bedrock and the location under consideration, $u_r(x, z, t)$:

$$u(x, z, t) = u_b(x, t) + u_r(x, z, t) \quad (3)$$

The following assumptions are made at this point regarding the layer response to the random incident motion:

(i) The incident random waves impinge the bedrock-layer interface at such angles that their propagation within the layers can be assumed to be vertical. This assumption serves as a first approximation, since it simplifies the wave propagation patterns in layered media, and is commonly used in the consideration of the effects of layers on seismic ground motions (e.g., [24]). Furthermore, it can be reasoned that, because the angle of transmission of body waves from the bedrock to the surface layer is steep and can be as steep as 90° [22], the propagation of the waveforms within the layer can be considered vertical.

(ii) The relative displacement $u_r(x, z, t)$ can be represented by the product of the generalized coordinate $u^*(x, t)$, and an assumed mode shape $\psi(z)$, that satisfies the geometric boundary conditions $\psi(0) = 1$ (at the ground surface) and $\psi(H) = 0$ (at the bedrock-layer

interface):

$$u_r(x, z, t) = u^*(x, t)\psi(z) \quad (4)$$

The assumed mode shape takes the form [11]:

$$\psi(z) = \cos\left(\frac{\pi z}{2H}\right) \quad (5)$$

which corresponds to the normalized first mode shape of a single, homogeneous, infinite, horizontal layer over a rigid bedrock (e.g., [20]). This consideration approximates the layer response by that of a single-degree-of-freedom oscillator with random characteristics, as will be shown later in the derivation. It is noted that this simplification eliminates the effects of higher modes present in a layered half-space, but captures the dominant layer response; it is generally acceptable that the site responds with a dominant frequency to seismic excitations (e.g., [25]). It is also noted that, with the enforcement of the boundary condition $\psi(H) = 0$, the model does not consider properly the effect of the layers on the total motion at the bedrock-layer interface; thus, the present approach is valid only for the estimation of surface ground motion characteristics.

For clarity purposes, it is also mentioned that the layer characteristics and the parameters affecting the incident motion at the bedrock-layer interface, such as source effects and random inhomogeneities along the path of the waves in the bedrock, are statistically independent quantities.

With the aforementioned considerations, the forces acting on an infinitesimal soil element within the layers are determined from [20]:

$$F_I(x, z, t) = -\rho(x, z) \frac{\partial^2 u(x, z, t)}{\partial t^2} dx dz = -\rho(x, z) \ddot{u}(x, z, t) dx dz \quad (6)$$

and

$$F_R(x, z, t) = \frac{\partial}{\partial z} \left[G(x, z) \frac{\partial u_r(x, z, t)}{\partial z} \right] dx dz \quad (7)$$

in which, $F_I(x, z, t)$ and $F_R(x, z, t)$ are the inertia and restoring force for the element, respectively. Through the principle of virtual work, i.e.,

$$\delta W = \int_0^H (F_I + F_R) \delta u_r = 0 \quad (8)$$

in which, $\delta u_r = \psi(z) \delta u^*(x, t)$, since $\psi(z)$ is the given shape function, the equation of motion becomes:

$$\ddot{u}^*(x, t) + [\omega^*(x)]^2 u^*(x, t) = -\beta \ddot{u}_b(x, t) \quad (9)$$

in which, $\omega^*(x)$ is the predominant layer natural frequency determined from Eqs. 1, 2, 6, 7 and 8 as:

$$\omega^*(x) = \sqrt{-\frac{\int_0^H \frac{\partial}{\partial z} [G(x, z) \psi'(z)] \psi(z) dz}{\int_0^H \rho(x, z) [\psi(z)]^2 dz}} = \sqrt{\frac{(1 + f_G(x)) \int_0^H G_z(z) [\psi'(z)]^2 dz}{(1 + f_\rho(x)) \int_0^H \rho_z(z) [\psi(z)]^2 dz}} \quad (10)$$

and β is the participation factor (Eqs. 2, 6, 7 and 8):

$$\beta = \frac{\int_0^H \rho(x, z) \psi(z) dz}{\int_0^H \rho(x, z) [\psi(z)]^2 dz} = \frac{\int_0^H \rho_z(z) \psi(z) dz}{\int_0^H \rho_z(z) [\psi(z)]^2 dz} \quad (11)$$

An approximate equivalent damping ratio, $\zeta^*(x)$, is then introduced in Eq. 9 to account for the energy loss due, but not necessarily exclusively, to the hysteretic behaviour of the soil under dynamic loading. Thus, the equation of motion becomes:

$$\ddot{u}^*(x, t) + 2\zeta^*(x) \omega^*(x) \dot{u}^*(x, t) + [\omega^*(x)]^2 u^*(x, t) = -\beta \ddot{u}_b(x, t) \quad (12)$$

The predominant natural frequency $\omega^*(x)$ and the equivalent damping ratio $\zeta^*(x)$ fluctuate randomly along x ; this fluctuation results from the stochasticity in the layer characteristics (Eqs. 1 and 2) and can, alternatively, be expressed as:

$$\omega^*(x) = \omega_0 [1 + \omega(x)] \quad (13)$$

$$\zeta^*(x) = \zeta_0 [1 + \zeta(x)] \quad (14)$$

in which, ω_0 and ζ_0 are the mean values of $\omega^*(x)$ and $\zeta^*(x)$, respectively, and $\omega(x)$ and $\zeta(x)$ are homogeneous stochastic fields with zero mean and corresponding standard deviations $\sigma_{\omega\omega}$ and $\sigma_{\zeta\zeta}$. It is noted that, since the approach is applicable to sites without

dramatic changes in their topography, the variability of both $\omega^*(x)$ and $\zeta^*(x)$ around their mean values is small; consequently, the standard deviations $\sigma_{\omega\omega}$ and $\sigma_{\zeta\zeta}$ of their random fluctuations, $\omega(x)$ and $\zeta(x)$, are small quantities.

The solution to the differential equation of motion (Eq. 12) is:

$$u^*(x, t) = -\beta \int_{-\infty}^{+\infty} h(x, \tau) \ddot{u}_b(x, t - \tau) d\tau \quad (15)$$

in which, $h(x, \tau)$ is the impulse response function:

$$h(x, \tau) = \begin{cases} \frac{1}{\omega^*(x) \sqrt{1 - [\zeta^*(x)]^2}} e^{-\zeta^*(x) \omega^*(x) \tau} \sin[\omega^*(x) \sqrt{1 - [\zeta^*(x)]^2} \tau] & \text{for } \tau \geq 0 \\ 0 & \text{for } \tau < 0 \end{cases} \quad (16)$$

Once $u^*(x, t)$ is determined, the seismic motions on the ground surface ($z = 0$) can be evaluated from:

$$u(x, z = 0, t) = u_b(x, t) + u^*(x, t) \quad (17)$$

which is essentially a repetition of Eq. 3 with the consideration that $\psi(0) = 1$.

$u^*(x, t)$ (Eq. 15) is determined as follows: The impulse response function $h(x, \tau)$ of Eq. 16 is expanded into a Taylor series around $\omega^*(x) = \omega_0$ and $\zeta^*(x) = \zeta_0$, and results (for $\tau \geq 0$) in:

$$\begin{aligned} h(x, \tau) \Big|_{\substack{\omega^*(x) = \omega_0 \\ \zeta^*(x) = \zeta_0}} &= \frac{e^{-\zeta_0 \omega_0 \tau}}{\omega_0 \sqrt{1 - \zeta_0^2}} \left[\sin \omega_0 \sqrt{1 - \zeta_0^2} \tau \right. \\ &+ \omega(x) \left(-\sin \omega_0 \sqrt{1 - \zeta_0^2} \tau - \zeta_0 \omega_0 \tau \sin \omega_0 \sqrt{1 - \zeta_0^2} \tau \right. \\ &\quad \left. \left. + \omega_0 \sqrt{1 - \zeta_0^2} \tau \cos \omega_0 \sqrt{1 - \zeta_0^2} \tau \right) \right. \\ &+ \zeta(x) \left(\frac{\zeta_0^2}{1 - \zeta_0^2} \sin \omega_0 \sqrt{1 - \zeta_0^2} \tau - \zeta_0 \omega_0 \tau \sin \omega_0 \sqrt{1 - \zeta_0^2} \tau \right. \\ &\quad \left. \left. - \frac{\zeta_0 \omega_0 \tau}{\sqrt{1 - \zeta_0^2}} \cos \omega_0 \sqrt{1 - \zeta_0^2} \tau \right) \right] \end{aligned} \quad (18)$$

Neglecting terms of order three and higher (i.e., $O(\zeta_0 \sigma_{\omega\omega}^2)$, $O(\zeta_0^2 \sigma_{\omega\omega}^2)$, $O(\zeta_0^2 \sigma_{\zeta\zeta}^2)$, etc.), due to smallness of ζ_0 , $\sigma_{\omega\omega}$ and $\sigma_{\zeta\zeta}$, and considering the statistical independence between the layer characteristics ($\omega(x)$ and $\zeta(x)$) and the incident motion at the bedrock-layer interface ($u_b(x, t)$), one can obtain, after lengthy but straight-forward algebraic manipulations, the cross spectral density of the relative ground displacement as:

$$S_{u^*u^*}(\xi, \omega) = \beta^2 \omega^4 \left[|H(\omega_0, \zeta_0, \omega)|^2 + 4\omega_0^4 R_{\omega\omega}(\xi) |H(\omega_0, \zeta_0, \omega)|^4 \right] S_{u_b u_b}(\xi, \omega) \quad (19)$$

in which, $R_{\omega\omega}(\xi)$ is the autocorrelation function of $\omega(x)$ (Eq. 13), and represents the fluctuation of the predominant frequency of the layer around its mean value. In Eq. 19, the frequency response function $H(\omega_0, \zeta_0, \omega)$ is given by:

$$H(\omega_0, \zeta_0, \omega) = \frac{1}{\omega_0^2 - \omega^2 + 2i\zeta_0\omega_0\omega} \quad (20)$$

with $i = \sqrt{-1}$, and $S_{u_b u_b}(\xi, \omega)$ is the cross spectral density of the incident motion at the bedrock-layer interface.

The cross spectral density of the total ground surface displacement is determined from Eqs. 17, 18 and 19, again after lengthy but straight-forward algebraic manipulations, as:

$$\begin{aligned} S_{uu}(\xi, \omega) = & [(\omega_0^4 + (2\beta + 4\zeta_0^2 - 2)\omega_0^2\omega^2 + (\beta - 1)^2\omega^4) |H(\omega_0, \zeta_0, \omega)|^2 \\ & + 4\beta^2\omega_0^4\omega^4 R_{\omega\omega}(\xi) |H(\omega_0, \zeta_0, \omega)|^4] S_{u_b u_b}(\xi, \omega) \end{aligned} \quad (21)$$

The corresponding power spectral density of the motions is obtained from Eq. 21 by setting the separation distance equal to zero, ($\xi = 0$), as:

$$\begin{aligned} S_{uu}(\omega) = & [(\omega_0^4 + (2\beta + 4\zeta_0^2 - 2)\omega_0^2\omega^2 + (\beta - 1)^2\omega^4) |H(\omega_0, \zeta_0, \omega)|^2 \\ & + 4\beta^2\omega_0^4\omega^4 \sigma_{\omega\omega}^2 |H(\omega_0, \zeta_0, \omega)|^4] S_{u_b u_b}(\omega) \end{aligned} \quad (22)$$

in which, $S_{u_b u_b}(\omega) = S_{u_b u_b}(\xi = 0, \omega)$, is the power spectrum of the incident motion. It is noted that, for a participation factor equal to one ($\beta = 1$, i.e., simple single-degree-of-freedom oscillator) and for deterministic values of the soil properties, Eq. 22 reduces to the well known Kanai-Tajimi spectrum [15], [31].

The parameters β , ω_0 , $R_{\omega\omega}(\xi)$, $\sigma_{\omega\omega}$, and ζ_0 in Eqs. 21 and 22 depend on the soil properties, and are evaluated in the following subsection for an example site. The description for the cross and power spectral densities of the incident motion at the bedrock-layer interface (Eqs. 21 and 22) are discussed in Section 3.

2.2 Stochastic characteristics of the ground

Consider the profile of an example site over a length of 1200m shown in Fig. 1. For simplicity, it is considered that the stochasticity in the soil characteristics results from variability in the depth of six sublayers ($M = 6$) consisting the 70m deep surface layer. The soil characteristics are constant within each sublayer and given in Table 1, and the sublayer boundaries are approximated by stepped lines as shown in Fig. 1. The cross sectional area is then divided into sixty vertical subsections each with dimensions 20m \times 70m. From the layer thickness (Fig. 1) and the soil material properties (Table 1), the predominant layer frequency $\omega^*(x_n)$, $n = 1, 2, \dots, 60$ can be computed by an extension of Okamoto's equation [21]:

$$\omega^*(x_n) = \frac{\pi}{2} \frac{1}{\sum_{j=1}^M \frac{H_j(x_n)}{v_{s_j}(x_n)}} \quad (23)$$

in which, $H_j(x_n)$ and $v_{s_j}(x_n)$ are the depth and shear wave velocity, respectively, of sublayer j at location x_n . The mean value and standard deviation of the sample data (Eq. 23) can be determined using standard techniques (e.g., Ref. [4]). For the particular example of Fig. 1 and Table 1, the mean predominant frequency of the layer becomes $\omega_0 = 5.64$ rad/sec with a corresponding standard deviation of $\sigma_{\omega\omega} = 0.101$.

The sample spatial correlation function for $\omega(x)$ (Eq. 13) is calculated by interpreting each sample as a realization of the stochastic process using the following equation:

$$\tilde{R}_{\omega\omega}(\xi_k) = \frac{1}{N-k} \sum_{n=1}^{N-k} \left[\frac{\omega^*(x_n + \xi_k) - \omega_0}{\omega_0} \right] \left[\frac{\omega^*(x_n) - \omega_0}{\omega_0} \right] \quad (24)$$

where N is the total number of soil vertical subsections ($N = 60$ for this example). In order to avoid a small averaging number $N - k$ in Eq. 24, the longest separation distance used was $\xi_k = 600m$. The resulting spatial correlation function, normalized by the variance $\sigma_{\omega\omega}^2$, is presented in Fig. 2. Later in this work, a closed form approximation for the spatial correlation function will be necessary so that the behaviour of the spatial variability is analytically reproduced, and the seismic ground strains are estimated. The analytical

approximation for $\tilde{R}_{\omega\omega}(\xi_k)$ is:

$$R_{\omega\omega}(\xi) = \sigma_{\omega\omega}^2 f_{\omega\omega}(\xi) \quad (25)$$

in which, $f_{\omega\omega}(\xi)$, the normalized spatial correlation function, ought to be consistent with the variability of the data at the site, and satisfy the following conditions: (i) it ought to be symmetric around $\xi = 0$ (homogeneity requirement); and (ii) its first and second derivatives ought to exist and assume finite values at $\xi = 0$, so that the evaluation of strains based on the expression is feasible. It is noted, that these two conditions impose that $f'_{\omega\omega}(0) = 0$. For the present example the mathematical expression used for $f_{\omega\omega}(\xi)$ is:

$$f_{\omega\omega}(\xi) = [1 - 2(\frac{\xi}{b_\omega})^2] e^{-(\frac{\xi}{b_\omega})^2} \quad (26)$$

in which, b_ω is the scale of correlation. The value of b_ω is determined in such a way that $R_{\omega\omega}(\xi)$ (Eq. 25) becomes zero for the same value of the separation distance ξ that produces a zero value for $\tilde{R}_{\omega\omega}(\xi)$ (Eq. 24); in this case, $\xi \approx 110m$ for $\tilde{R}_{\omega\omega}(\xi) = 0$ (Fig. 2), and, thus, $b_\omega = 155.56m$. The analytical spatial correlation function (Eqs. 25 and 26), normalized by the layer frequency variance, is also plotted in Fig. 2. Alternative expressions for the normalized autocorrelation function can be found in, e.g., Ref. [10].

In the absence of more refined data for the damping coefficient, it is assumed that $\zeta_0 = 0.20$ for the soft soil site (low predominant frequency) of the present example. $\zeta_0 = 0.20$, 0.40 and 0.60 are commonly used values for damping coefficients for soft, intermediate and firm soil conditions [8], [13], [31].

The participation factor β is obtained from Eq. 11 through integration of deterministic functions, which involve the mean value of the soil mass of the layer and the shape function. In this example, the soil mass is constant in each sublayer, but the sublayers' thickness fluctuates. A gross estimate for the participation factor can be obtained if the soil mass is averaged over all sublayers and the integration performed over the entire layer thickness,

i.e.,

$$\beta = \frac{\int_0^H \psi(z) dz}{\int_0^H \psi^2(z) dz} = \frac{4}{\pi} = 1.273 \quad (27)$$

Alternatively, β can be determined from the mean value of the participation factor obtained through the application of Eq. 11 to each vertical subsection, i.e.,

$$\beta(x_n) = \frac{\int_0^H \rho(x_n, z) \psi(z) dz}{\int_0^H \rho(x_n, z) [\psi(z)]^2 dz} = \frac{\sum_{i=1}^M \rho_i \int_{h_i}^{h_i+H_i} \psi(z) dz}{\sum_{i=1}^M \rho_i \int_{h_i(x_n)}^{h_i(x_n)+H_i(x_n)} [\psi(z)]^2 dz} \quad (28)$$

in which, M is the number of soil sublayers, ρ_i is the soil mass in sublayer i (Table 1), $H_i(x_n)$ is the thickness of the sublayer at location x_n (Fig. 1), and $h_i(x_n) = \sum_{l=1}^{i-1} H_l(x_n)$ for $i > 1$ and $h_1(x_n) = 0$. The mean value of the participation factors resulting from Eq. 28 is $\beta = 1.302$, a value not significantly different from the gross estimate of Eq. 27. In the following, the mean value of $\beta = 1.302$ is used. It is noted that this value represents the actual participation factor for all vertical subsections; the variance of the participation factor obtained from the data of Eq. 28 was 9.4×10^{-5} .

The power spectral density of the total surface motions normalized with respect to that of the incident motion (Eq. 22) is shown in Fig. 3. As expected, its power is contained in the vicinity of the mean value of the layer predominant frequency and its shape resembles that of the Kanai-Tajimi spectrum.

3 Seismic motion spatial correlation structure

As indicated in the Introduction, the spatial variation of seismic ground motions results from the apparent propagation of the waveforms on the ground surface and the differences in their shape at the various locations. Commonly, the more well understood wave passage effect is considered independently of the other spatial variability causes. The main descriptor of the remaining spatial variability causes is the coherence, defined as the absolute value of the cross spectrum of the motions at two recording stations divided by the square root of

the product of the power spectra at the two stations. Coherence estimates are insensitive to the amplitude differences of the motions at the various locations [29]. Consequently, the variability in the motions described by the coherence is attributed mainly to their phase differences [1], i.e., coherence represents essentially random phase fluctuations. It is noted that, although coherence describes phase variability, it is not associated with the (deterministic) apparent propagation of the motions on the ground surface; quadrant-symmetric space-time random fields [35], as most coherence models are, represent motions that are superpositions of standing waves [37]. The power spectra of the motions, which are proportional to the square of the amplitude, are, generally, assumed to be the same at all locations, an assumption also made implicitly in Eq. 22.

In the present notation, the spatial variation of seismic ground motions is expressed as:

$$\gamma_{sv}(\xi, \omega) = \frac{S_{**}(\xi, \omega)}{S_{**}(\xi = 0, \omega)} \quad (29)$$

and their coherence as:

$$\gamma_{coh}(\xi, \omega) = \frac{|S_{**}(\xi, \omega)|}{S_{**}(\xi = 0, \omega)} \quad (30)$$

in which, $*$ \equiv u for the surface motions, or $*$ \equiv u_b for the incidence motions.

The incident motion coherence and the apparent propagation of the waveforms are estimated in the following subsection, and followed by the evaluation of the total surface motion spatial correlation structure.

3.1 Spatial variation of incident motions

Since stationarity is assumed throughout the analysis, the incident motion at the bedrock-layer interface is described by its cross spectral density between two stations at a distance ξ apart from each other as (Eq. 29):

$$S_{u_b u_b}(\xi, \omega) = S_{u_b u_b}(\omega) \gamma_{b.sv}(\xi, \omega) \quad (31)$$

in which, $S_{u_b, u_b}(\omega)$, the power spectral density of the incident motion (displacement) at the bedrock-layer interface, is considered to be the same at all locations, and $\gamma_{b.sv}(\xi, \omega)$ indicates the spatial variation of that motion.

In Eq. 31, the incident motion power spectral density can be approximated by the commonly used seismological spectra [14]. The spatial variation of the motions $\gamma_{b.sv}(\xi, \omega)$ is decomposed into a term describing loss of coherence, $\gamma_{b.coh}(\xi, \omega)$, and a term representing propagation, $\gamma_{b.prop}(\xi, \omega, c)$ with c indicating velocity, as:

$$\gamma_{b.sv}(\xi, \omega) = \gamma_{b.coh}(\xi, \omega) \gamma_{b.prop}(\xi, \omega, c) \quad (32)$$

Since it has been suggested that the finite source effect on the spatial variability is not significant [29], the loss of coherence of the incident motions will result from the scattering of the waves as they travel from the source to the bedrock-layer interface, which can be approximated by stochastic wave propagation [27], [33]. For the shear wave window analyzed herein, the incident motion coherence is approximated by the model of Luco and Wong [19], which is based on the analysis of shear waves propagating a distance R through a random medium:

$$\begin{aligned} \gamma_{b.coh}(\xi, \omega) &= e^{-\left(\frac{\eta \omega \xi}{v_{rm}}\right)^2} = e^{-\alpha^2 \omega^2 \xi^2} \\ \eta &= \mu \left(\frac{R}{r_0}\right)^{1/2} \quad \alpha = \frac{\eta}{v_{rm}} \end{aligned} \quad (33)$$

v_{rm} is an estimate for the elastic shear wave velocity in the random medium (bedrock), r_0 the scale length of random inhomogeneities along the path, and μ^2 a measure of the relative variation of the elastic properties in the medium. α , the incoherence parameter, controls the exponential decay of the function; the higher the value of α , the higher the loss of coherence as separation distance and frequency increase. With appropriate choices for the incoherence parameter, the model has been shown to fit the spatial variation of recorded data, and has been used extensively by researchers in their evaluation of the seismic response analysis of lifelines (e.g., [8], [19], [36], [38], [39]). In these approaches, Eq. 33 has been used for the

description of the spatial coherence of the surface motions, whereas herein it represents the coherence of the incident excitation at the bedrock-layer interface. This does not necessarily constitute an inconsistency: The expression is based on shear wave propagation through random media, an approximation which may be valid for the propagation of the waves from the source to the ground surface or from the source to the bedrock-layer interface; Der Kiureghian [7] has also recently used Eq. 33 for the description of the bedrock motion coherence. It is also noted that the degree of loss of coherence in Eq. 33 is the same with increasing frequency and separation distance. This behaviour is not consistent with some recent observations, that suggest that the decay of coherence with frequency may differ from its decay with separation distance [29]. The present methodology can accommodate these recent developments: when alternative formulations, that reproduce these observations, become available, they can be easily incorporated in Eqs. 31 and 32 instead of Luco and Wong's expression.

The apparent propagation of the motions is described in spatial variability expressions (Eqs. 29 and 32) by:

$$\gamma_{b.prop}(\xi, \omega, c) = e^{-i\omega\xi/c} \quad (34)$$

which represents the frequency dependent correlation function of a unidirectional random wave propagating with constant velocity c [35]. The consideration that the entire seismic ground motion propagates with a constant velocity is valid, since only the window of the strong S-wave motion is considered. This observation has been verified from analyses of recorded data for the estimation of the spatial variability (e.g., Ref. [12]), and also from the slowness spectra evaluation of broad-band body waves [30], [41]. It is noted that c (in Eq. 34) is the apparent propagation velocity of the incident motion at the bedrock-layer interface, which is a function of the shear wave velocity in the bedrock, v_{rm} , and the angle of incidence of waves at the interface. As indicated in Section 2, it is considered that the waves impinge the interface at such angles, that their propagation within the layer can be

considered vertical.

3.2 Spatial variation of surface motions

With the considerations of Sections 2 and 3.1, the cross spectral density of the total surface motion becomes:

$$S_{uu}(\xi, \omega) = [\mathcal{H}_1(\beta, \omega_0, \zeta_0, \omega) + R_{\omega\omega}(\xi) \mathcal{H}_2(\beta, \omega_0, \zeta_0, \omega)] S_{u_b u_b}(\omega) e^{-\alpha^2 \omega^2 \xi^2} e^{-i \frac{\omega \xi}{c}} \quad (35)$$

in which,

$$\mathcal{H}_1(\beta, \omega_0, \zeta_0, \omega) = (\omega_0^4 + (2\beta + 4\zeta_0^2 - 2) \omega_0^2 \omega^2 + (\beta - 1)^2 \omega^4) |H(\omega_0, \zeta_0, \omega)|^2 \quad (36)$$

$$\mathcal{H}_2(\beta, \omega_0, \zeta_0, \omega) = 4\beta^2 \omega_0^4 \omega^4 |H(\omega_0, \zeta_0, \omega)|^4 \quad (37)$$

Equation 35 incorporates the contributions of both the incident motion variability and the layer stochasticity to the total correlation structure of the surface motions. In order to analyze these effects separately, their contributions are isolated from one another:

In the absence of the layers the variability of the surface motions becomes identical to that of the incident motion (Eq. 32). The variation with frequency of the term representing loss of coherence in the incident motion ($e^{-\alpha^2 \omega^2 \xi^2}$ from Eq. 33) at separation distances of 40, 100, 200, and 500m is presented in Fig. 4; α is equal to 2.5×10^{-4} sec/m, a median value between the ones suggested by Luco and Wong [19] from their analyses of actual earthquake data ($2 - 3 \times 10^{-4}$ sec/m). The wave passage term in the incident motion spatial variation ($e^{-i \frac{\omega \xi}{c}}$ from Eq. 34) introduces a phase difference in the seismic ground motions at various stations, the value of which is determined from:

$$\phi_b(\xi, \omega) = \arctan \frac{\Im(e^{-i \frac{\omega \xi}{c}})}{\Re(e^{-i \frac{\omega \xi}{c}})} = -\frac{\omega \xi}{c} \quad (38)$$

with \Re and \Im indicating the real and imaginary part, respectively; Eq. 38 represents the deterministic phase of a broad band S-wave propagating with constant velocity c .

In order to isolate the effect of the layer stochasticity from that of the incident motion in the total spatial variability, it is assumed that the bedrock motion is fully coherent with $c \rightarrow \infty$ (i.e., $S_{u_b u_b}(\xi, \omega) = S_{u_b u_b}(\omega)$ in Eq. 31). For fully coherent incidence motions, the resulting surface motion random field is quadrant-symmetric, and, thus, the stochasticity in the layers affects the coherence of the motions according to (Eqs. 30 and 35):

$$\gamma_{l.coh}(\xi, \omega) = \frac{[\mathcal{H}_1(\beta, \omega_0, \zeta_0, \omega) + R_{\omega\omega}(\xi) \mathcal{H}_2(\beta, \omega_0, \zeta_0, \omega)]}{[\mathcal{H}_1(\beta, \omega_0, \zeta_0, \omega) + \sigma_{\omega\omega}^2 \mathcal{H}_2(\beta, \omega_0, \zeta_0, \omega)]} \quad (39)$$

The contribution of the layer stochasticity to the spatial variation of the motions (Eq. 39) at separation distances of 40, 100, 200, and 500m is presented in Fig. 5; the actual values of the spatial correlation function $\tilde{R}_{\omega\omega}(\xi)$ (Eq. 24) were used in the figure. The correlation structure in Fig. 5 is different from the one expected in spatial variability (i.e., exponential decay with both separation distance and frequency). The expression decays close to the frequency of the first mode of the layers and assumes a constant value close to perfect correlation as frequency increases. The behaviour of the correlation in Fig. 5 is realistic: The layer responds to the incident excitation as a series of single-degree-of-freedom systems with slightly varying, correlated frequency. For input motion frequencies close to the mean natural frequency of the “oscillators”, the response of the systems is affected by the variability in the value of this natural frequency, and results in loss of correlation. As the exciting frequencies increase past the natural frequency of the systems, the actual value of the natural frequency (for small variabilities) ceases to affect the response significantly.

The overall coherence (incident motion coherence and layer stochasticity) in the spatial variation of the surface motions is expressed as (Eqs. 30, 33 and 39):

$$\gamma_{coh}(\xi, \omega) = \gamma_{b.coh}(\xi, \omega) \gamma_{l.coh}(\xi, \omega) \quad (40)$$

and is presented in Fig. 6. It is noted from the figure that the overall shape of the total coherence is controlled by that of the incident motion; the layer stochasticity results in a decrease in the correlation close to the mean value of the natural frequency of the layer.

This should be expected, since the total coherence of the surface motions is the product of the incident motion coherence and the one resulting from the layer stochasticity.

The overall agreement of the spatial coherence with and without site effects is consistent with previous observations at various array sites, which indicate that the site variability may not particularly influence the overall correlation structure of the total motion [25], [26]. It also justifies the use of smoothly decaying spatial coherence models with parameters obtained from surface records (such as Luco and Wong's model) to describe the coherence of the incident motions in the present approach. However, the drop in the correlation at the predominant frequency of the layers is distinguishable. This drop-in-coherence behaviour observed in Figs. 5 and 6 has also been noted by Kanasewich [16], who suggested that site resonances can be identified from holes in the coherence spectra of motions at adjacent locations, and by Cranswick [5], who further indicated that perturbations with small deviations in the layer characteristics will produce the greatest changes in the response functions, and, since coherence is a measure of similarity of the motions, it will be low at the resonant frequencies. Thus, the present approach incorporates site effects in the spatial correlation structure of the motions that are consistent with observations, but have not been taken into account before in its estimates. Generally, it is assumed that the site contribution results from the response of individual, statistically independent soil columns with different characteristics. Accordingly, the site contribution does not affect coherence, but produces a deterministic phase difference in the surface motion correlation [7]. Clearly, the deterministic phase difference is caused by the delays in the arrival of the waves from the bedrock to the ground surface due to their propagation through different layers. The present approach approximates the soil columns transmitting the bedrock excitation to the ground surface by single-degree-of-freedom systems with similar, correlated characteristics. The time delay in the arrival of the waves from the interface to the ground surface is incorporated in the model through the layer predominant frequency (Eq. 12): an incident

impulse acceleration at the bedrock-layer interface at $t = 0$ would produce a maximum response on the ground surface at approximately $t = \frac{1}{4}(\frac{2\pi}{\omega_0})$, $\frac{2\pi}{\omega_0}$ representing the period of oscillation. The layer stochasticity causes random fluctuations in the arrival of the waves from the bedrock to the surface, and, thus, affects the coherence -random phase variability- of the motions. The apparent propagation (deterministic phase) of the surface motions is controlled by that of the incident motion, since vertical propagation is considered within the layer. It is emphasized that the present methodology is applicable to sites with no dramatic changes in their topography, for which the homogeneity assumption for the layer variability is valid. For sites with spatial characteristics that deviate significantly from constant mean values, the spatial homogeneity assumption ought to be waived; in this case, the layer stochasticity would affect both the coherence and the apparent propagation (deterministic phase) of the motions.

Based on Eqs. 29, 35 and 39, the spatial variation of the surface motions becomes:

$$\gamma_{sv}(\xi, \omega) = \frac{[\mathcal{H}_1(\beta, \omega_0, \zeta_0, \omega) + R_{\omega\omega}(\xi) \mathcal{H}_2(\beta, \omega_0, \zeta_0, \omega)]}{[\mathcal{H}_1(\beta, \omega_0, \zeta_0, \omega) + \sigma_{\omega\omega}^2 \mathcal{H}_2(\beta, \omega_0, \zeta_0, \omega)]} e^{-\alpha^2 \omega^2 \xi^2} e^{-i\frac{\omega\xi}{c}} \quad (41)$$

4 Evaluation of seismic ground strains

Seismic strains resulting on the surface of the stochastic layer are evaluated as follows: The cross correlation function of the seismic motions on the ground surface is defined as:

$$R_{uu}(\xi, \tau) = \int_{-\infty}^{+\infty} S_{uu}(\xi, \omega) e^{i\omega\tau} d\omega \quad (42)$$

From the above expression, the variance of the horizontal seismic strains along the x -direction (direction of wave propagation on the ground surface) becomes:

$$\sigma_{\epsilon\epsilon}^2 = \left[-\frac{\partial^2 R_{uu}(\xi, \tau)}{\partial \xi^2} \right]_{\substack{\xi=0 \\ \tau=0}} = -\left[\int_{-\infty}^{+\infty} \frac{\partial^2 S_{uu}(\xi, \omega)}{\partial \xi^2} d\omega \right]_{\xi=0} \quad (43)$$

and that of the seismic ground velocities (particle velocities):

$$\sigma_{vv}^2 = \left[-\frac{\partial^2 R_{uu}(\xi, \tau)}{\partial \tau^2} \right]_{\substack{\xi=0 \\ \tau=0}} = \left[\int_{-\infty}^{+\infty} \omega^2 S_{uu}(\xi, \omega) d\omega \right]_{\xi=0} \quad (44)$$

The square-root of the variance (root-mean-square) of a random quantity provides information on its mean maximum value, since rms values are proportional to the mean maximum ones [6].

The evaluation of seismic ground strains (Eq. 43) requires the integration of the second derivative with respect to ξ of the cross correlation of the motions at $\tau = 0$, which becomes (Eqs. 21, 31, 32 and 42):

$$R_{uu}(\xi, \tau = 0) = \int_{-\infty}^{+\infty} [\mathcal{H}_1(\beta, \omega_0, \zeta_0, \omega) + R_{\omega\omega}(\xi) \mathcal{H}_2(\beta, \omega_0, \zeta_0, \omega)] \times S_{\ddot{u}_b \ddot{u}_b}(\omega) e^{-\alpha^2 \omega^2 \xi^2} e^{-i \frac{\omega \xi}{c}} d\omega \quad (45)$$

in which, $\mathcal{H}_1(\beta, \omega_0, \zeta_0, \omega)$, and $\mathcal{H}_2(\beta, \omega_0, \zeta_0, \omega)$ are given by Eqs. 36 and 37, respectively. Since both the value and the derivatives of the spatial correlation function $R_{\omega\omega}(\xi)$ are needed at $\xi = 0$ in Eqs. 43 and 45, its analytical approximation (Eq. 25) is required. These derivatives, for any assumed correlation function expression $f_{\omega\omega}(\xi)$, take the form:

$$R_{\omega\omega}(0) = \sigma_{\omega\omega}^2; \quad R'_{\omega\omega}(0) = 0; \quad R''_{\omega\omega}(0) = \sigma_{\omega\omega}^2 f''_{\omega\omega}(0) \quad (46)$$

The substitution of Eq. 46 into Eqs. 43 and 45 yields the variance of the seismic ground strains:

$$\sigma_{\epsilon\epsilon}^2 = \int_{-\infty}^{+\infty} [\omega^2 (2\alpha^2 + (\frac{1}{c})^2) (\mathcal{H}_1 + \sigma_{\omega\omega}^2 \mathcal{H}_2) - \sigma_{\omega\omega}^2 f''_{\omega\omega}(0) \mathcal{H}_2] S_{\ddot{u}_b \ddot{u}_b}(\omega) d\omega \quad (47)$$

in which, the dependence of \mathcal{H}_1 and \mathcal{H}_2 on β , ω_0 , ζ_0 and ω has been omitted for simplicity. With the assumption that $S_{\ddot{u}_b \ddot{u}_b}(\omega)$, the power spectral density of the incident motion acceleration, is a slowly varying function of frequency, and noting that both $|H(\omega_0, \zeta_0, \omega)|^2$ and $|H(\omega_0, \zeta_0, \omega)|^4$ peak close to $\omega = \omega_0$, an approximation for the variance of the ground strains is found to be:

$$\sigma_{\epsilon\epsilon}^2 = \{\omega_0^2 [2\alpha^2 + (\frac{1}{c})^2] [\beta^2 (1 + \frac{\sigma_{\omega\omega}^2}{2\zeta_0^2}) + 4\zeta_0^2] - \frac{\beta^2 \sigma_{\omega\omega}^2 f''_{\omega\omega}(0)}{2\zeta_0^2} (1 + 4\zeta_0^2)\} \frac{\pi}{2\zeta_0 \omega_0^3} S_{\ddot{u}_b \ddot{u}_b}(\omega_0) \quad (48)$$

The variance of the seismic velocity at the ground surface can also be evaluated through a similar procedure. Equations 36, 37, 44 and 46 lead to:

$$\sigma_{vv}^2 = \int_{-\infty}^{+\infty} \omega^2 (\mathcal{H}_1 + \sigma_{\omega\omega}^2 \mathcal{H}_2) S_{u_b u_b}(\omega) d\omega \quad (49)$$

which, with the same approximations used in the evaluation of the seismic strains, yields:

$$\sigma_{vv}^2 = \{\omega_0^2 [\beta^2 (1 + \frac{\sigma_{\omega\omega}^2}{2\zeta_0^2}) + 4\zeta_0^2]\} \frac{\pi}{2\zeta_0 \omega_0^3} S_{\ddot{u}_b \ddot{u}_b}(\omega_0) \quad (50)$$

Equations 48 and 50 then result in the following estimate for the rms seismic ground strain in terms of the rms ground velocity:

$$\frac{\sigma_{\epsilon\epsilon}}{\sigma_{vv}} = \sqrt{[2\alpha^2 + (\frac{1}{c})^2] - \frac{\beta^2 \sigma_{\omega\omega}^2 f''_{\omega\omega}(0)}{2\zeta_0^2 \omega_0^2} \frac{(1 + 4\zeta_0^2)}{[\beta^2 (1 + \frac{\sigma_{\omega\omega}^2}{2\zeta_0^2}) + 4\zeta_0^2]}} \quad (51)$$

The normalized spatial correlation function of the present example (Eq. 26) yields $f''_{\omega\omega}(0) = -\frac{6}{b_\omega^2}$, and Eq. 51 takes the form:

$$\frac{\sigma_{\epsilon\epsilon}}{\sigma_{vv}} = \sqrt{[2\alpha^2 + (\frac{1}{c})^2] + \frac{3\beta^2 \sigma_{\omega\omega}^2}{\zeta_0^2 \omega_0^2 b_\omega^2} \frac{(1 + 4\zeta_0^2)}{[\beta^2 (1 + \frac{\sigma_{\omega\omega}^2}{2\zeta_0^2}) + 4\zeta_0^2]}} \quad (52)$$

Figure 7 presents the rms seismic strain ($\sigma_{\epsilon\epsilon}$) normalized with respect to the rms ground velocity (σ_{vv}) as function of the apparent propagation velocity of the motions on the ground surface. Three variations of the seismic strains are presented in the figure: the first corresponds to the incident motion effects only, i.e.,

$$\frac{\sigma_{\epsilon\epsilon}}{\sigma_{vv}} = \sqrt{2\alpha^2 + (\frac{1}{c})^2} \quad (53)$$

the second corresponds only to site effects ($\alpha = 0$ in Eq. 52), and the third incorporates the contributions of both the incident motion variability and the layer stochasticity (Eq. 52). The shape of the ground strain vs. apparent propagation velocity variability in Fig. 7 is consistent with simulations of seismic ground strains and velocities [38], and with analyses of actual seismic strains from recorded data during the 1971 San Fernando earthquake [22]:

The variation of seismic strains at low velocities is not affected by the loss of coherence in the motions; this is consistent with the commonly used approximation in engineering practice when surface waves dominate in the motions, namely that seismic strains are equal to the ground (particle) velocity divided by the apparent propagation velocity of the motions. When body waves dominate -as is the case for the strong motion shear wave window-, the effect of the loss of coherence in the motions on seismic ground strains becomes significant (Fig. 7). For the soft soil profile considered herein, Fig. 7 indicates that the contribution of the layer stochasticity essentially controls the seismic strains. This effect was not obvious from the spatial variability of the surface ground motions (Fig. 6), although not altogether unexpected, since the layer stochasticity contribution occurs at the dominant soil frequency (Eq. 48). As expected, the combined effect of the bedrock motion and layer stochasticity yields higher strains (Fig. 7).

5 Summary and conclusion

The evaluation of the seismic response of lifelines, such as pipelines and bridges, requires estimates for the spatial variation of the seismic ground motions at the site. Such estimates are difficult to obtain at sites where recorded seismic data from dense arrays are not available.

An approach for the analytical evaluation of the spatial variation of the seismic ground motions at sites that can be approximated by a stochastic layer overlaying a bedrock has been presented. As is commonly the case in the estimation of the spatial variation, only direct shear waves have been considered. The model presented incorporates the basic factors that contribute to the spatial variation of seismic ground motions and the assumptions made in the approach are consistent with observations from recorded data and well-established approximations. It has been assumed that the spatial variation of the incident motion at the bedrock-layer interface can be described by its spatial coherence and its apparent

propagation. The spatial coherence of the incident motion is described by the expression derived by Luco and Wong [19] from the analysis of shear wave propagation through random media. A constant apparent propagation velocity for the broad-band shear waves along the interface has been utilized. The incident shear waves at the bedrock-layer interface were then assumed to propagate vertically through the stochastic layer and the site response was approximated by that of one-degree-of-freedom oscillators with random properties.

It was shown that the shape of the spatial variation of the motions on the ground surface is controlled by that of the incident motion. The site contribution is concentrated in the vicinity of the predominant frequency of the layer and yields a drop in the value of the coherence. Such site effects, although observed, have not been incorporated before in spatial variability models. Seismic ground strains evaluated from the model suggested that the contribution of the site stochasticity can be significant: it essentially controls the strains at higher -body wave- apparent propagation velocities for the soft soil conditions considered herein. Since strains are the key parameter in the seismic response analysis of buried pipelines and are also indicative of the amplitude of differential displacements, which control the seismic quasi-static response of above-ground lifelines, the results of this analysis suggest that the effect of layer stochasticity cannot be neglected in the evaluation of the spatial variation of seismic ground motions.

The methodology developed herein provides an approximation for the spatial variation of the seismic ground motions that incorporates information on the soil profile at the site. In the absence of spatially recorded seismic data at a site, the spatially variable motions resulting from the model can be applied as input motions at the supports of above-ground and buried lifelines in their seismic resistant analysis and design.

6 Acknowledgments

This paper is dedicated to Professor Franz Ziegler of the Institut für Allgemeine Mechanik, Technische Universität Wien, Vienna, Austria, on the occasion of his 60th birthday. The study was supported by the US National Science Foundation (NSF) under Grant No. BCS-9114895. The writers wish to thank Dr. Michel Kahan of the Laboratoire des Matériaux et des Structures du Génie Civil, LCPC/CNRS, Champs sur Marne, France, and Dr. Paul Spudich of the US Geological Survey, Menlo Park, California, for insightful comments and valuable suggestions.

References

- [1] N.A. Abrahamson, "Generation of spatially incoherent strong motion time histories", *Proceedings, Tenth World Conference on Earthquake Engineering*, Madrid, Spain, 1992.
- [2] N.A. Abrahamson, J.F. Schneider and J.C. Stepp, "Spatial variation of strong ground motion for use in soil-structure interaction analyses", *Proceedings of the Fourth US-National Conference on Earthquake Engineering*, Palm Springs, CA, 1990.
- [3] N.A. Abrahamson, B.A. Bolt, R.B. Darragh, J. Penzien and Y.B. Tsai, "The SMART-1 Accelerograph array (1980-1987): A review", *Earthquake Spectra*, Vol. 3, pp. 263-287, 1987.
- [4] A. H-S. Ang and W.H. Tang *Probabilistic Concepts in Engineering Planning and Design. Volume I-Basic Principles*, John Wiley, New York, NY, 1975.
- [5] E. Cranswick, "The information content of high-frequency seismograms and the near-surface geologic structure of "hard rock" recording sites", *Pure and Applied Geophysics*, Vol. 128, pp. 333-363, 1988.
- [6] M. Berrah and E. Kausel, "Modified response spectrum model for the design of structures subjected to spatially varying seismic excitations", Research Report R90-2, Department of Civil Engineering, Massachusetts Institute of Technology, Cambridge, MA, 1989.
- [7] A. Der Kiureghian, "A coherency model for spatially varying ground motions", *Earthquake Engineering and Structural Dynamics*, Vol. 25, pp. 99-111, 1996.

- [8] A. Der Kiureghian and A. Neuenhofer, "A response spectrum method for multiple-support seismic excitations", Earthquake Engineering Research Center, Report No. UCB/EERC-91-08, University of California, Berkeley, CA, 1991.
- [9] T. Harada, "Probabilistic modeling of spatial variation of strong earthquake ground displacement", *Proceedings of the Eighth World Conference on Earthquake Engineering*, San Francisco, CA, pp. 605-612, 1984.
- [10] T. Harada and M. Shinozuka, "Ground deformation spectra", *Proceedings of the Third US-National Conference on Earthquake Engineering*, Charleston, SC, pp. 2191-2202, 1986.
- [11] T. Harada and M. Shinozuka, "Stochastic analysis of spatial variability of seismic ground deformation", in *Recent Advances in Lifeline Earthquake Engineering*, T. Ariman, M. Hamada, A.C. Singhal and A.S. Cakmak, editors, Elsevier Publishing Company, Amsterdam, The Netherlands, 1987.
- [12] R.S. Harichandran and E.H. Vanmarcke, "Stochastic variation of earthquake ground motion in space and time", *Journal of the Engineering Mechanics Division*, Vol. 112, pp. 154-174, 1986.
- [13] A. Hindy and M. Novak, "Pipeline response to random ground motion", *Journal of the Engineering Mechanics Division, ASCE*, Vol. 106, pp. 339-360, 1980.
- [14] W.B. Joyner and D.M. Boore, "Measurement, characterization and prediction of strong ground motion", in *Earthquake Engineering and Soil Dynamics II- Recent Advances in Ground Motion Evaluation*, Geotechnical Special Publication No. 20, J.L. von Thun ed., ASCE, New York, NY, 1988.
- [15] K. Kanai, "An empirical formula for the spectrum of strong earthquake motion", *Proceedings of the Second World Conference on Earthquake Engineering*, Tokyo and Kyoto, Japan, 1960.
- [16] E.R. Kanasewich, *Time Sequence Analysis in Geophysics*, The University of Alberta Press, Edmonton, Alberta, Canada, 1981.
- [17] C.H. Loh, "Analysis of the spatial variation of seismic waves and ground movements from SMART-1 data", *Earthquake Engineering and Structural Dynamics*, Vol. 13, pp. 561-581, 1985.
- [18] C.H. Loh, J. Penzien and Y.B. Tsai, "Engineering Analysis of SMART-1 array accelerograms", *Earthquake Engineering and Structural Dynamics*, Vol. 10, pp. 575-591, 1982.

- [19] J.E. Luco and H.L. Wong, "Response of a rigid foundation to a spatially random ground motion", *Earthquake Engineering and Structural Dynamics*, Vol. 14, pp. 891-908, 1986.
- [20] N.M. Newmark and E. Rosenblueth, *Fundamentals of Earthquake Engineering*, Prentice Hall Inc. Englewood Cliffs, NJ, 1971.
- [21] S. Okamoto, *Introduction to Earthquake Engineering*, University of Tokyo Press, Tokyo, Japan, 1984.
- [22] M.J. O'Rourke, G. Castro and N. Centola, "Effects of seismic wave propagation upon buried pipelines", *Earthquake Engineering and Structural Dynamics*, Vol. 8, pp. 455-467, 1980.
- [23] M.J. O'Rourke, G. Castro and I. Hossain, "Horizontal strain due to seismic waves", *Journal of Geotechnical Engineering, ASCE*, Vol. 110, pp. 1173-1187, 1984.
- [24] P.B. Schnabel, J. Lysmer and H.B. Seed, "SHAKE: a computer program for earthquake response analysis of horizontally layered sites", *Earthquake Engineering Research Center Report No. EERC-72/12*, University of California, Berkeley, CA, 1972.
- [25] J.F. Schneider, N.A. Abrahamson, P.G. Somerville and J.C. Stepp, "Spatial variation of ground motion from EPRI's dense accelerograph array at Parkfield, California", *Proceedings of the Fourth US-National Conference on Earthquake Engineering*, Palm Springs, CA, 1990.
- [26] J.F. Schneider, J.C. Stepp and N.A. Abrahamson "The spatial variation of earthquake ground motion and effects of local site conditions", *Proceedings of the Fourth US-National Conference on Earthquake Engineering*, Palm Springs, CA, 1990.
- [27] K. Sobczyk, *Stochastic wave propagation*, PWN-Polish Scientific Publishers, Warszawa, Poland, 1984.
- [28] P.G. Somerville, G.P. McLaren, C.K. Saikia and D.V. Helmberger, "Site-specific estimation of spatial incoherence of strong ground motion", in *Earthquake Engineering and Soil Dynamics II- Recent Advances in Ground Motion Evaluation*, Geotechnical Special Publication No. 20, J.L. von Thun ed., ASCE, New York, NY, 1988.
- [29] P. Spudich, "Recent seismological insights into the spatial variation of earthquake ground motions", in *New Developments in Earthquake Ground Motion Estimation and Implications for Engineering Design Practice*, ATC 35-1, 1994.

- [30] P. Spudich and D. Oppenheimer, "Dense seismograph array observations of earthquake rupture dynamics", in *Earthquake Source Mechanics*, Geophysical Monograph 37, S. Das, J. Boatwright and C.H. Scholz, eds., American Geophysical Union, Washington, D.C., 1986.
- [31] H. Tajimi, "A statistical method for determining the maximum response of a building structure during an earthquake", *Proceedings of the Second World Conference on Earthquake Engineering*, Tokyo and Kyoto, Japan, 1960.
- [32] H. Tajimi, *Introduction to structural dynamics*, Corona-sha, Tokyo, Japan, 1964.
- [33] B.J. Uscinski, *The elements of wave propagation in random media*, McGraw-Hill, New York, NY, 1977.
- [34] E.H. Vanmarcke, editor, *Proceedings of the International Workshop on Spatial Variation of Earthquake Ground Motion*, National Center for Earthquake Engineering Research, Buffalo, NY, 1988.
- [35] E.H. Vanmarcke, *Random Fields. Analysis and Synthesis*, MIT Press, Cambridge, MA, 1983.
- [36] A. Zerva, "Response of multi-span beams to spatially incoherent seismic ground motions", *Earthquake Engineering and Structural Dynamics*, Vol.19, pp. 819-832,1990.
- [37] A. Zerva, "Seismic ground motion simulations from a class of spatial variability models", *Earthquake Engineering and Structural Dynamics*, Vol.21, pp.351-361,1992.
- [38] A. Zerva, "Spatial incoherence effects on seismic ground strains", *Probabilistic Engineering Mechanics*, Vol. 7, pp. 217-226, 1992.
- [39] A. Zerva, "Seismic loads predicted by spatial variability models", *Structural Safety*, Vol. 11, pp. 227-243, 1992.
- [40] A. Zerva, "On the spatial variation of seismic ground motions and its effects on lifelines", *Engineering Structures*, Vol. 16, pp. 534-546, 1994.
- [41] A. Zerva and O. Zhang, "Correlation patterns in characteristics of spatially variable seismic ground motions", *Earthquake Engineering and Structural Dynamics*, Vol. 26, pp. 19-39, 1997.

Table 1: Material properties of the site profile in Fig. 1

Layer	Soil Mass g/cm^3	Poisson Ratio	Shear Modulus kg^*/cm^2	Shear Wave Velocity m/sec
1 Sand	1.80	0.48	133.0	85.0
2 Sand	1.70	0.48	287.0	125.0
3 Clay	1.50	0.48	612.0	200.0
4 Gravel	1.90	0.48	2050.0	325.0
5 Sandstone	2.10	0.48	5360.0	500.0
6 Sandstone	2.20	0.48	14367.0	800.0

List of Figures

Figure 1 Cross section of the soil profile used in the numerical example. The vertical subsections are also shown in the **Figure**.

Figure 2 Spatial correlation functions for the predominant ground frequency of the stochastic layer using the actual soil data and the analytical approximation

Figure 3 Total surface motion (displacement) power spectral density, $S_{uu}(\omega)$, normalized with respect to the power spectrum of the incident motion, $S_{u_b u_b}(\omega)$

Figure 4 Variation of the spatial coherence of the incident motion [Luco and Wong's model] with frequency at separation distances of 40, 100, 200 and 500m

Figure 5 Variation of the spatial coherence due to layer stochasticity with frequency at separation distances of 40, 100, 200 and 500m

Figure 6 Variation of the total spatial coherence (incident motion and layer stochasticity) with frequency at separation distances of 40, 100, 200 and 500m

Figure 7 Variation of rms strain over rms ground velocity ($\sigma_{\epsilon\epsilon}/\sigma_{vv}$) with the apparent propagation velocity of the motions (c)

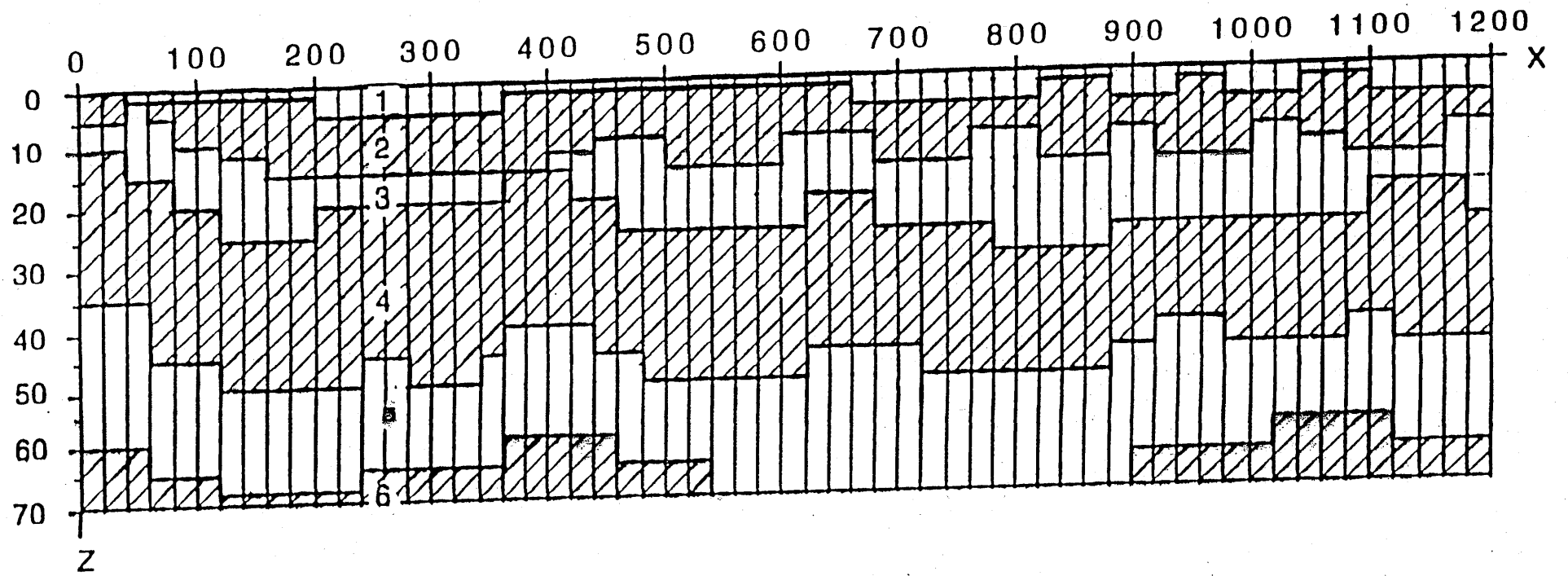


Figure 1

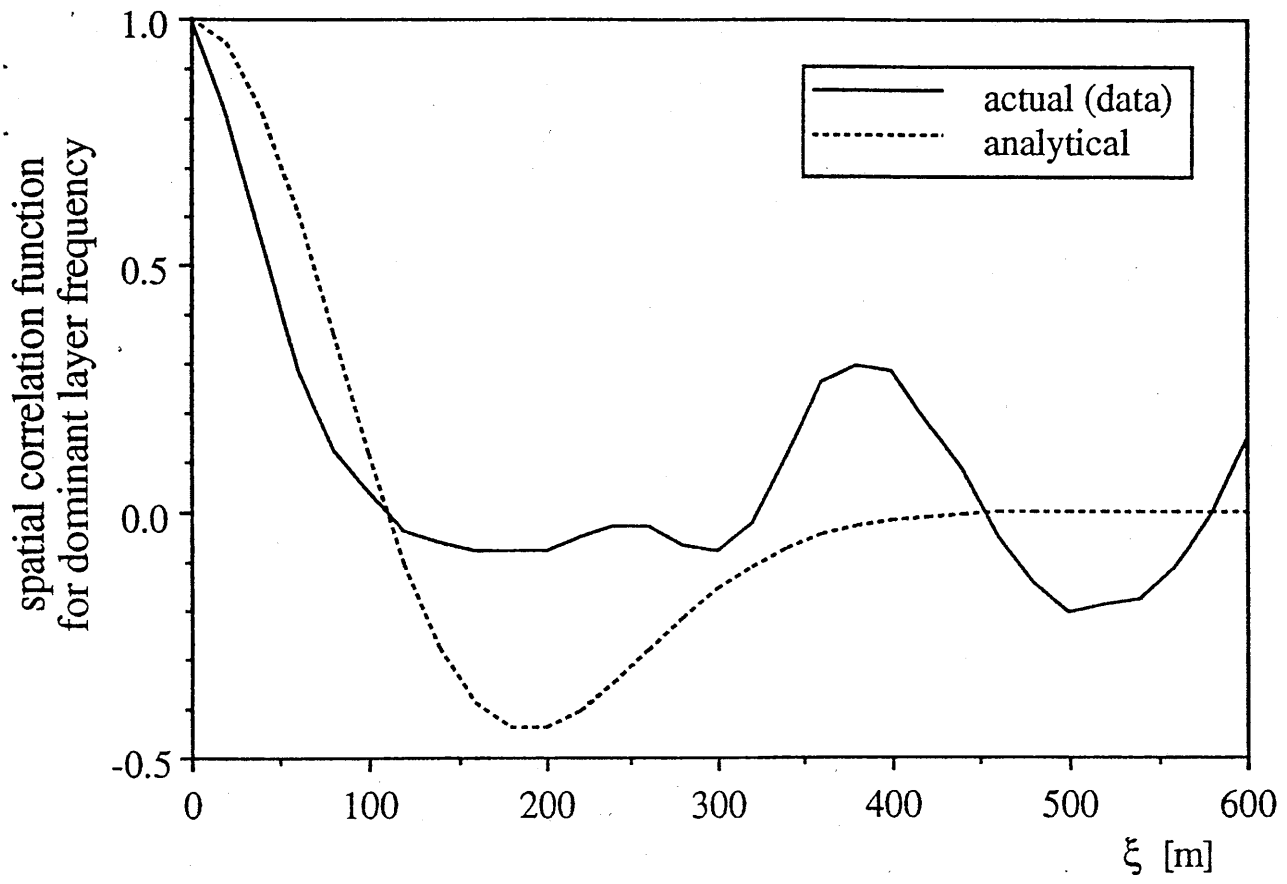


Figure 2

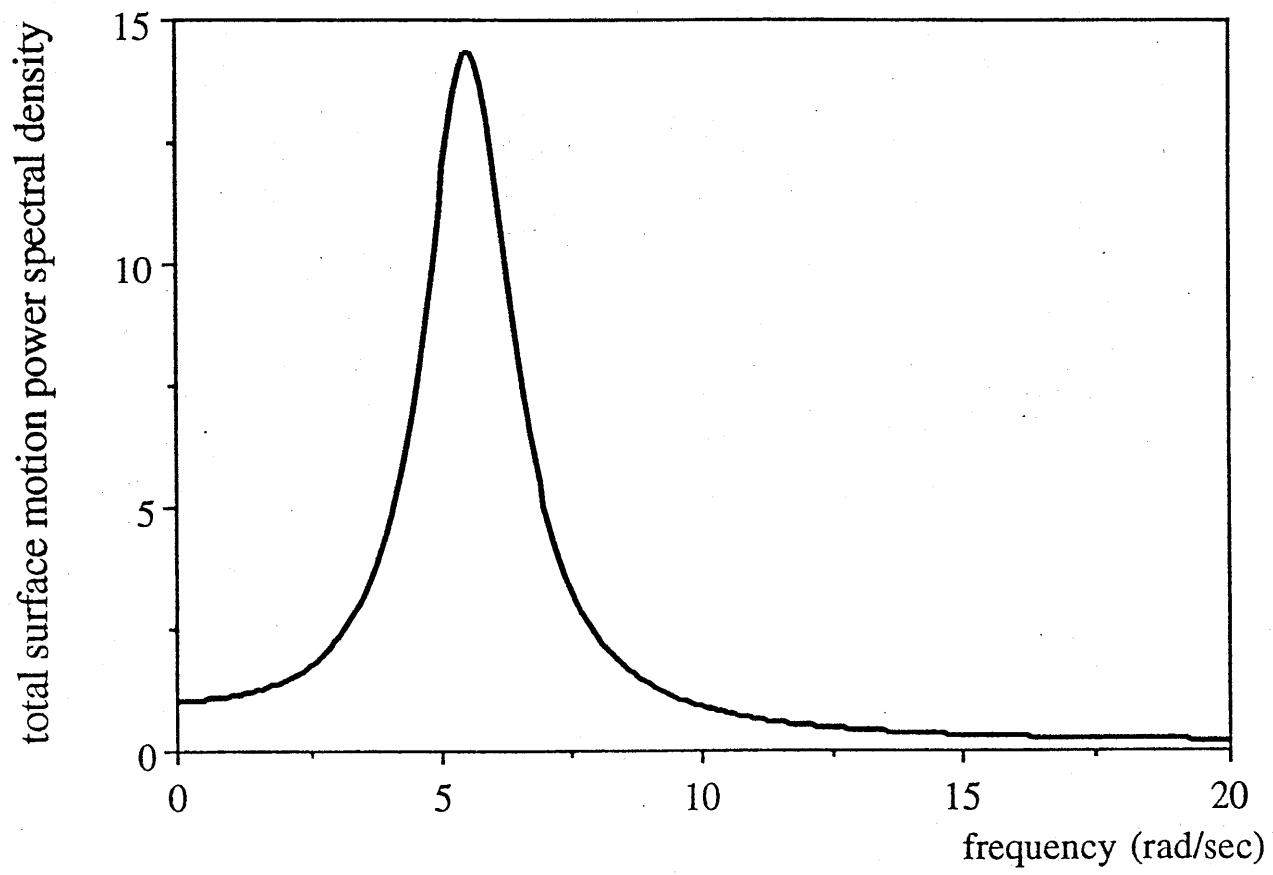


Figure 3

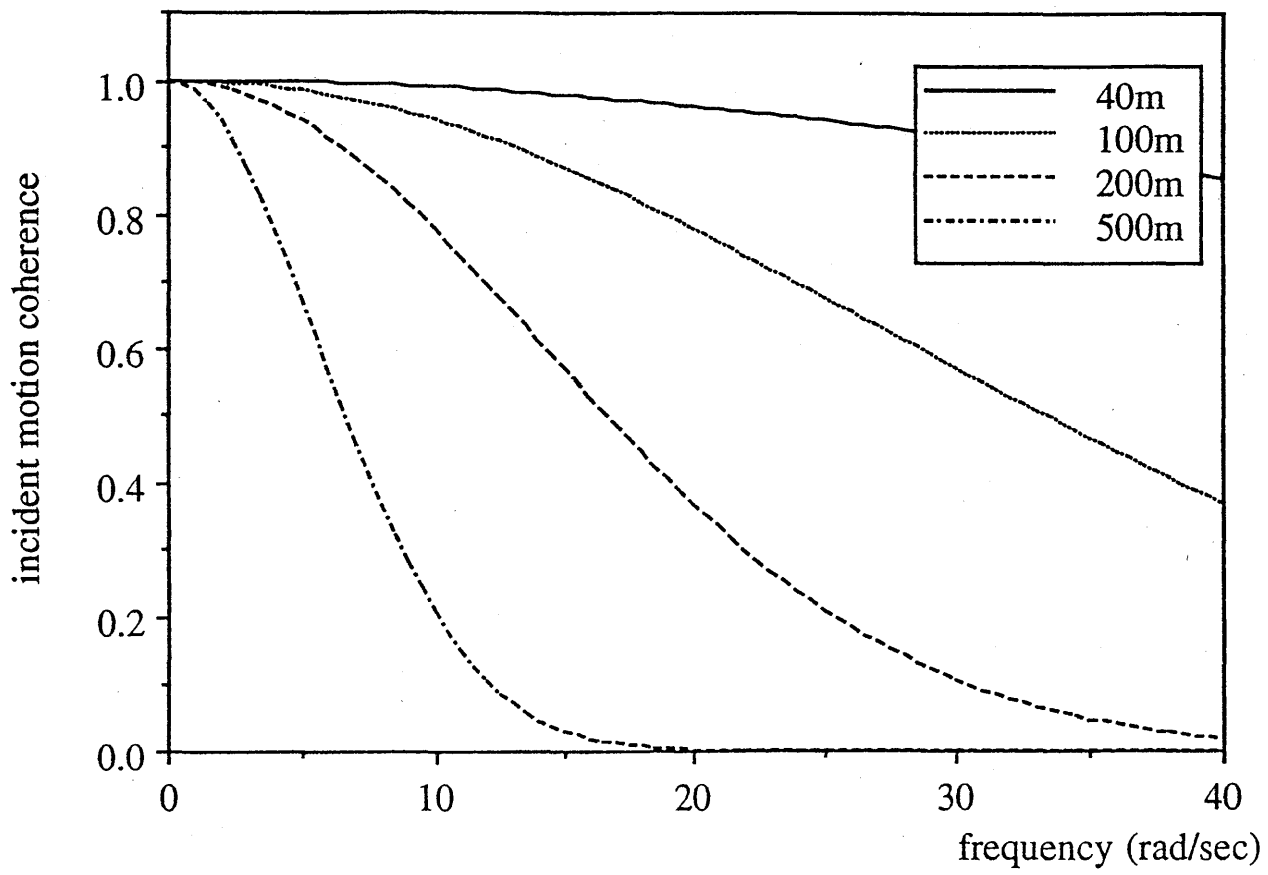


Figure 4

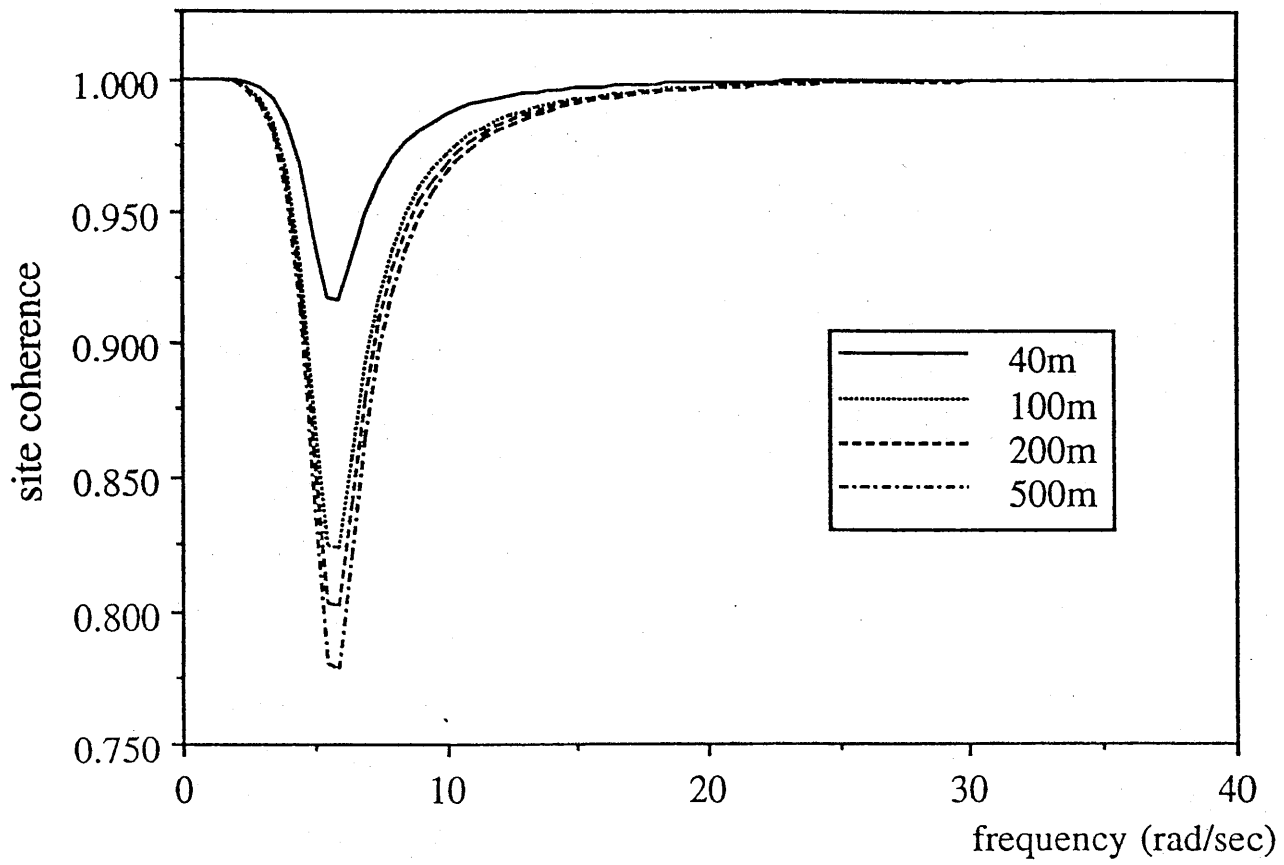


Figure 5

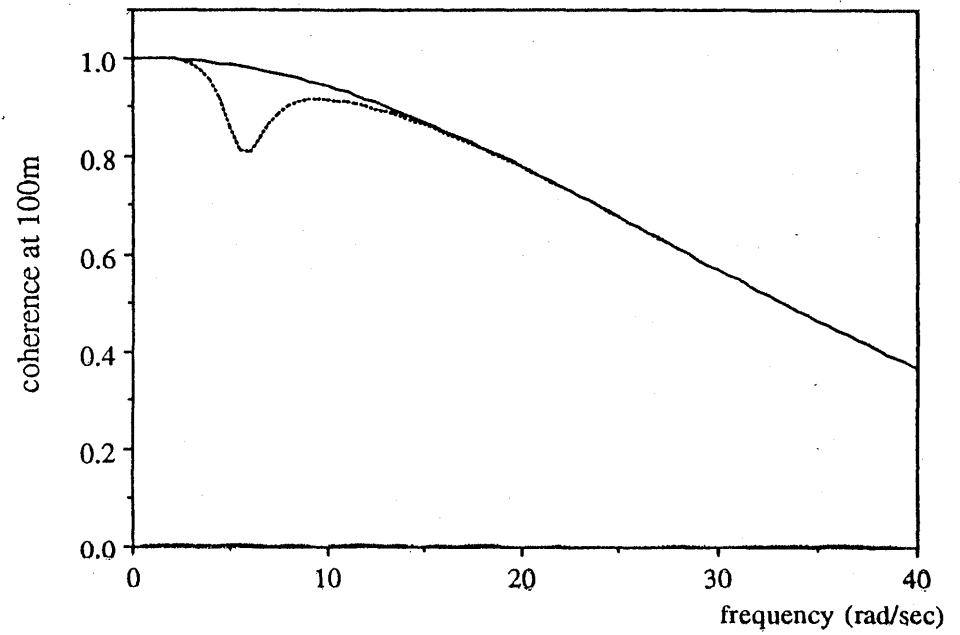
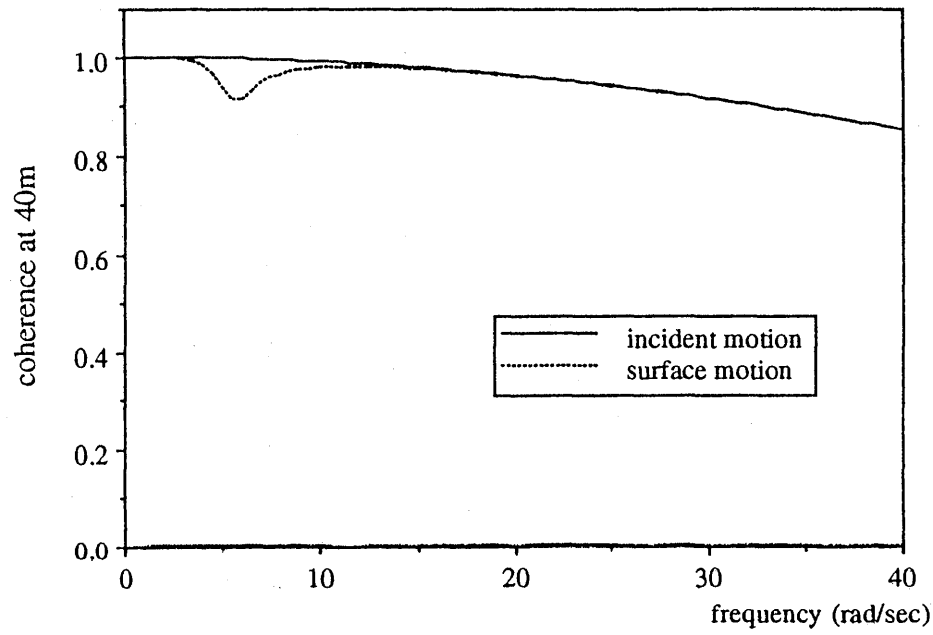
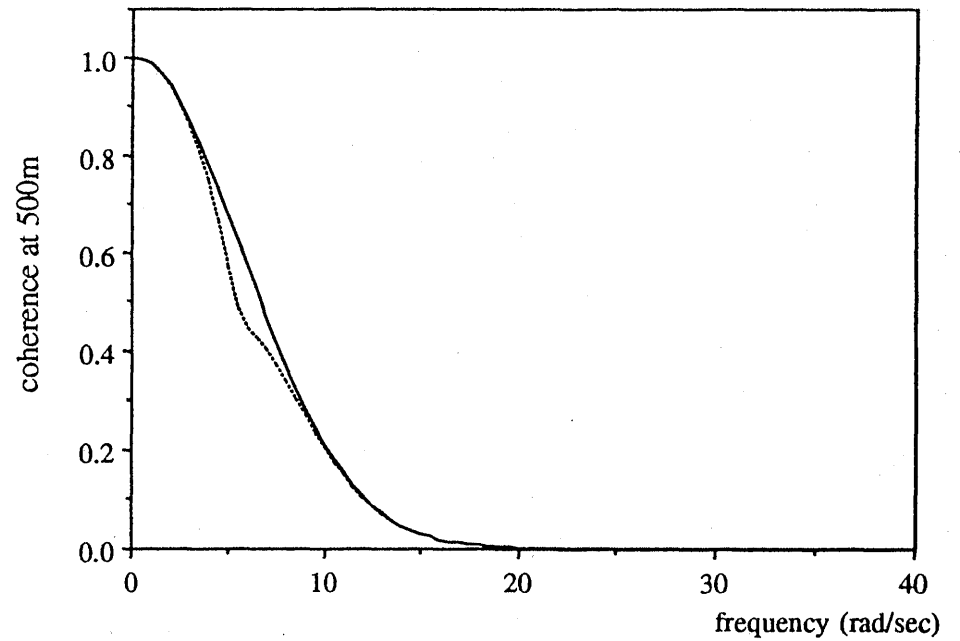
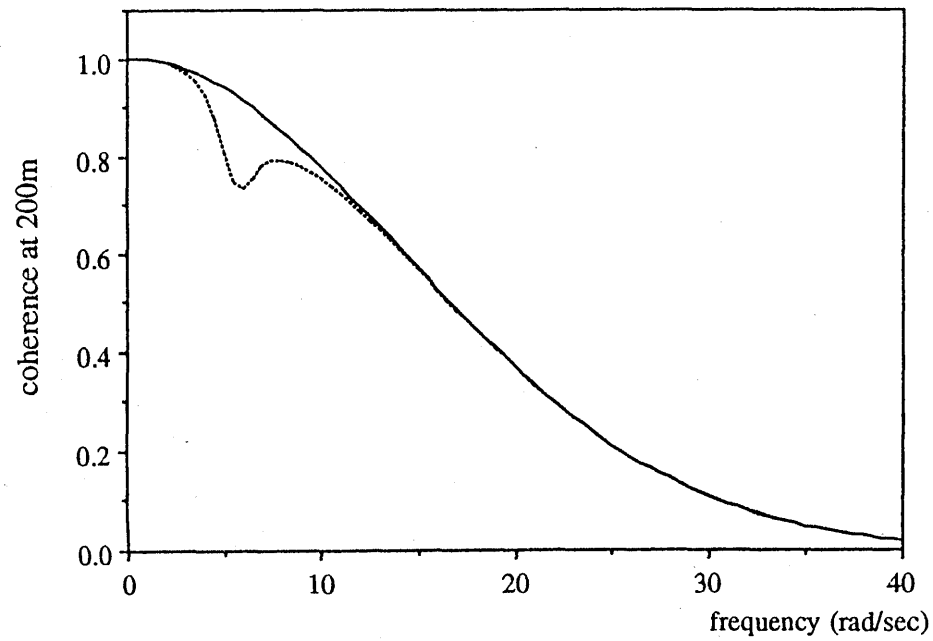


Figure 6



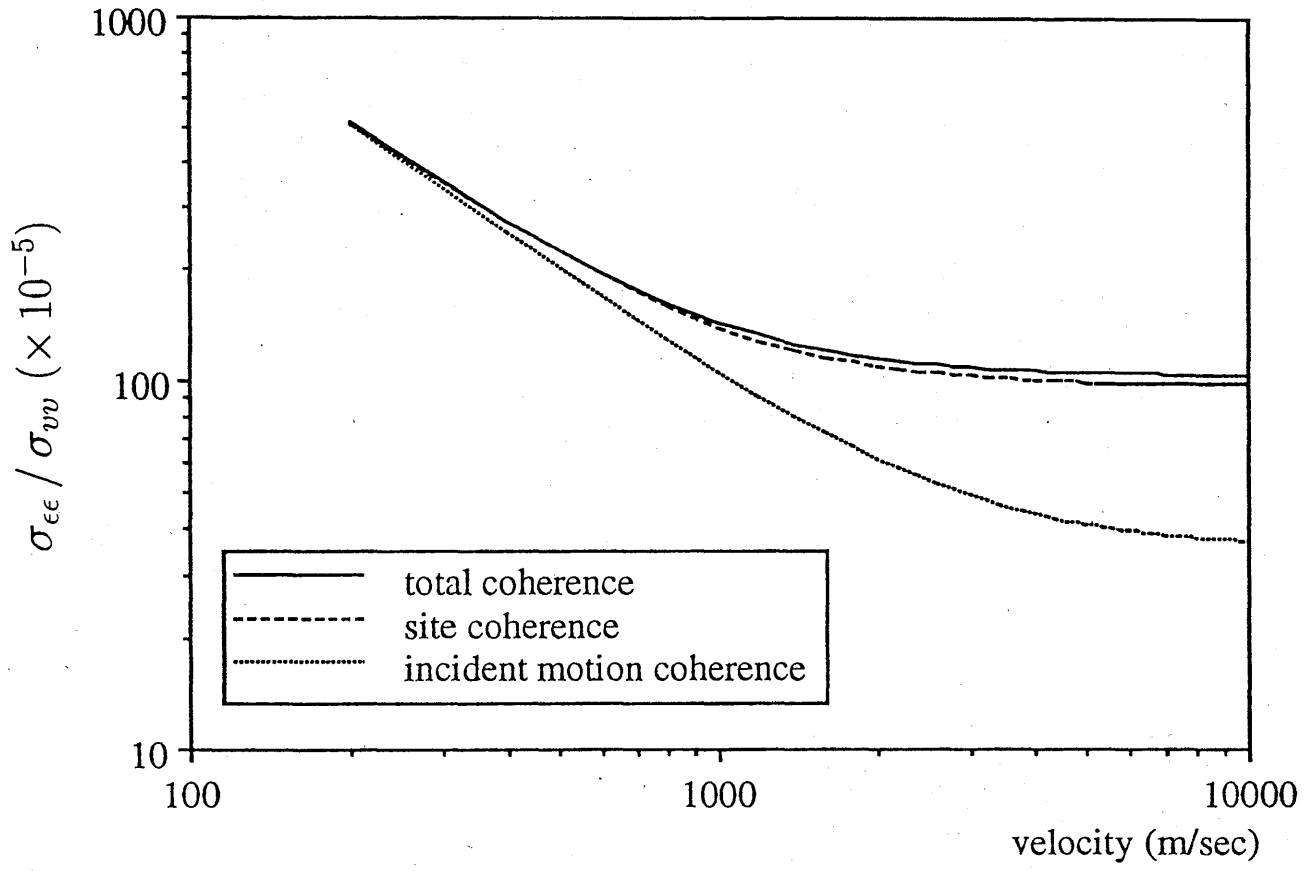


Figure 7